

Cite this: *Lab Chip*, 2012, **12**, 1768

www.rsc.org/loc

## COMMUNICATION

**“Fluidic batteries” as low-cost sources of power in paper-based microfluidic devices†**

Nicole K. Thom, Kimy Yeung, Marley B. Pillion and Scott T. Phillips\*

Received 4th February 2012, Accepted 12th March 2012

DOI: 10.1039/c2lc40126f

This communication describes the first paper-based microfluidic device that is capable of generating its own power when a sample is added to the device. The microfluidic device contains galvanic cells (that we term “fluidic batteries”) integrated directly into the microfluidic channels, which provides a direct link between a power source and an analytical function within the device. This capability is demonstrated using an example device that simultaneously powers a surface-mount UV LED and conducts an on-chip fluorescence assay.

Exceedingly low-cost, yet highly sensitive and selective diagnostic devices are needed for diagnosing disease in extremely resource-limited locations around the world.<sup>1</sup> One strategy for creating these types of devices involves pairing a reader<sup>2</sup> (e.g., a glucose reader or hand-held spectrophotometer) with a second device that contains the reagents for the assay. In contrast to this traditional approach, the World Health Organization (WHO) has put forth performance guidelines for ideal diagnostic devices for use in the developing world.<sup>3</sup> While these guidelines include typical considerations of cost, sensitivity, and selectivity, they differ from many standard approaches because, in part, they underscore the need for diagnostic devices that are equipment-free. This criterion suggests that an ideal diagnostic device for these settings would operate without the aid of readers, appended batteries (including button batteries), auxiliary stopwatches, or any other equipment that would be considered auxiliary to the diagnostic device.

Here we describe a step towards this type of ideal diagnostic by demonstrating an integrated source of power in a paper-based microfluidic device<sup>4</sup> for powering on-chip functions. This source of power (*i.e.*, fluidic batteries) provides sufficient power to illuminate a UV LED for on-chip fluorescence assays, and likely will be useful for powering electrochemical detection and separation schemes, optical readouts for assays, as well as other on-chip functions.

These fluidic batteries are configured such that the source of power is positioned in channels that are aligned (or adjacent) to an assay, which is an arrangement that simplifies the process of making

connections between the source of power and the operation that requires the power. Likewise, these fluidic batteries turn on only when the sample is added to the paper-based microfluidic device; hence, a single sample is used both for conducting an assay and for powering components that may be needed for the assay. Finally, the galvanic cells in the fluidic batteries can be tuned to achieve a desired current or potential, and can be adjusted to use the minimum quantity of electrolytes and electrodes needed for a particular application, thus minimizing the cost of the batteries and decreasing the hazardous waste associated with disposing of used paper-based microfluidic devices. These favourable attributes make fluidic batteries an attractive alternative to button batteries and auxiliary hand-held readers for point-of-care assays in resource-limited environments.

Fluidic batteries in paper-based microfluidic devices require four components (Fig. 1): (i) electrolytes (which are pre-deposited into defined hydrophilic regions of a device prior to assembling the device); (ii) electrodes (which are incorporated into air gaps in the patterned tape during assembly); (iii) salt bridges (one for each galvanic cell); and (iv) conductive connections (copper tape) between galvanic cells, and between galvanic cells and the device that is powered (*e.g.*, a LED). We used  $\text{AgNO}_3$  and  $\text{AlCl}_3$  as electrolytes for these fluidic batteries, and deposited them in a 3 : 1 ratio of Ag–Al per cell. We chose Ag and Al for initial demonstrations because the half reactions of  $\text{Al}/\text{Al}^{3+}$  and  $\text{Ag}/\text{Ag}^+$  give a theoretical potential of 2.4 V and transfer three electrons per cell, which is a reasonable starting point for achieving the current and potential that is needed to power surface-mount LEDs. The electrodes consisted of silver or aluminum metal shaped into either a square (1.5 mm × 1.5 mm; 250  $\mu\text{m}$  thick) or a disk (1.5 mm in diameter; 250  $\mu\text{m}$  thick), with the shape depending on the configuration of the galvanic cell. The salt bridges contained  $\text{NaNO}_3$  that was pre-deposited from a saturated aqueous solution and then dried in the appropriate layer of hydrophilic paper prior to assembling the device. The assembled microfluidic devices containing fluidic batteries have been stored for at least five weeks at 25 °C, open to the air, without loss in performance.<sup>5</sup> Moreover, the fluidic batteries contribute little to the overall materials cost for the paper microfluidic device<sup>6</sup> (a favourable attribute, given the cost constraints outlined by the WHO).

Fluidic batteries will be most useful for enabling a variety of point-of-care diagnostic assays if they can be tuned easily to access a range of current and voltage values. There are three easily adjusted factors that affect the maximum short circuit current ( $I_{\text{sc}}$ ) and open circuit voltage ( $V_{\text{oc}}$ ) values obtained from these fluidic batteries. (1) The

Department of Chemistry, The Pennsylvania State University, University Park, Pennsylvania 16802, USA. E-mail: sphillips@psu.edu; Fax: +814 865 5235; Tel: +814 867 2502

† Electronic supplementary information (ESI) available: Tables of data, experimental procedures, dimensions of devices. See DOI: 10.1039/c2lc40126f

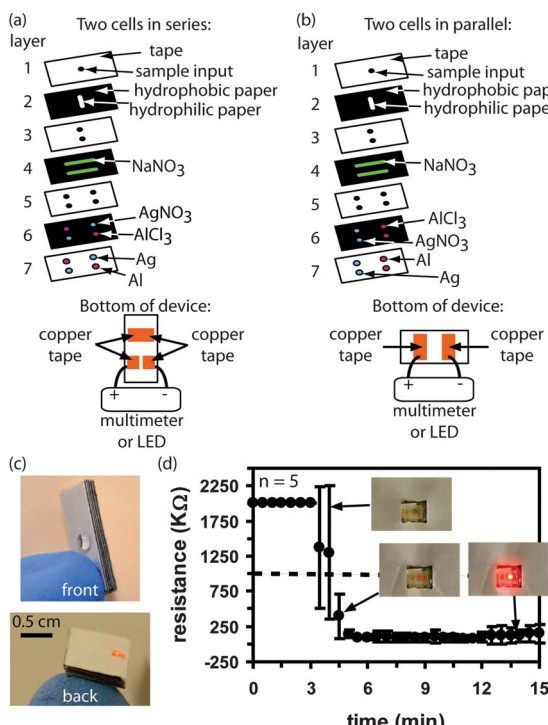


**Fig. 1** The design of fluidic batteries for providing power to paper-based microfluidic devices once a sample is added to the device. The fluidic batteries are made from galvanic cells that are incorporated into the microfluidic channels of the paper-based device. The number of galvanic cells can be varied, and can be linked in (a) series or (b) parallel. The black regions in even numbered layers are hydrophobic wax, while the white regions are hydrophilic paper. In odd numbered layers, the white regions are hydrophobic tape, while the black regions are hydrophilic paper. The examples shown in (a) and (b) do not contain regions for assays. (c) Photographs of the front and the back of a four-cell device (two cells in parallel and two of these groups in series). A red LED ( $\lambda_{\text{em}} = 630 \text{ nm}$ ) illuminates when the fluidic battery turns on. (d) A photoresistor was used to measure the intensity of light emitted by the red LED after a 10- $\mu\text{L}$  sample of water was added to the device. The intensity of light is approximately inversely proportional to the resistance measured with the photoresistor. The LED is illuminated at all points below the dotted line in (d). The measurements in (d) were repeated five times.

quantity of electrolytes in the cell: at least 9  $\mu\text{g}$  of Ag(I) is needed per half-cell in a four-cell battery to illuminate a red LED ( $\lambda_{\text{em}} = 630 \text{ nm}$ ) for 1.4 min (Fig. S7). (2) The number of cells: when the quantity of electrolytes is fixed at 33.3  $\mu\text{g}$  AlCl<sub>3</sub> and 127  $\mu\text{g}$  AgNO<sub>3</sub> per half-cell, then the  $V_{\text{oc}}$  and  $I_{\text{sc}}$  values range from 660  $\mu\text{A}$  and 1.3 V for one galvanic cell (Fig. S1) to 722  $\mu\text{A}$  and 5.0 V for a 16-cell battery (four cells in parallel, and four of these groups in series, Fig. S5) to 2.8 mA and 3.8 V for a 24-cell battery (eight cells in parallel, and three of these in series, Fig. S6).<sup>7</sup> (3) The arrangement of the cells in series or parallel (or both): for example, the two cells in series in Fig. 1a provide 520  $\mu\text{A}$  and 2.4 V, whereas the two cells in parallel in Fig. 1b provide 890  $\mu\text{A}$  and 1.3 V.

The duration of the maximum current and potential is dependent only on the rate with which the sample reaches and dissolves the electrolytes, and on the quantity of electrolytes per cell (Fig. S7). For example, a four-cell fluidic battery (2 cells in parallel, and two of these groups in series) that contains 9  $\mu\text{g}$  Ag(I) per cell (and a 3 : 1 ratio of

Ag-Al) powers the red LED for 1.4 min, whereas an identical device that contains 67  $\mu\text{g}$  Ag(I) powers the LED for 8.2 min.

Given the ability to generate a battery in a paper-based microfluidic device, we next sought to demonstrate the utility of this battery. Fig. 2 shows an example paper-based device that powers an integrated surface-mount UV LED. This LED is used in a proof-of-concept fluorescent assay that detects the enzyme  $\beta$ -D-galactosidase.<sup>8</sup>

Fig. 2c shows the assay reagent (7-(D-galactosyloxy)coumarin (**1**), which is non-fluorescent) as well as the products that are formed

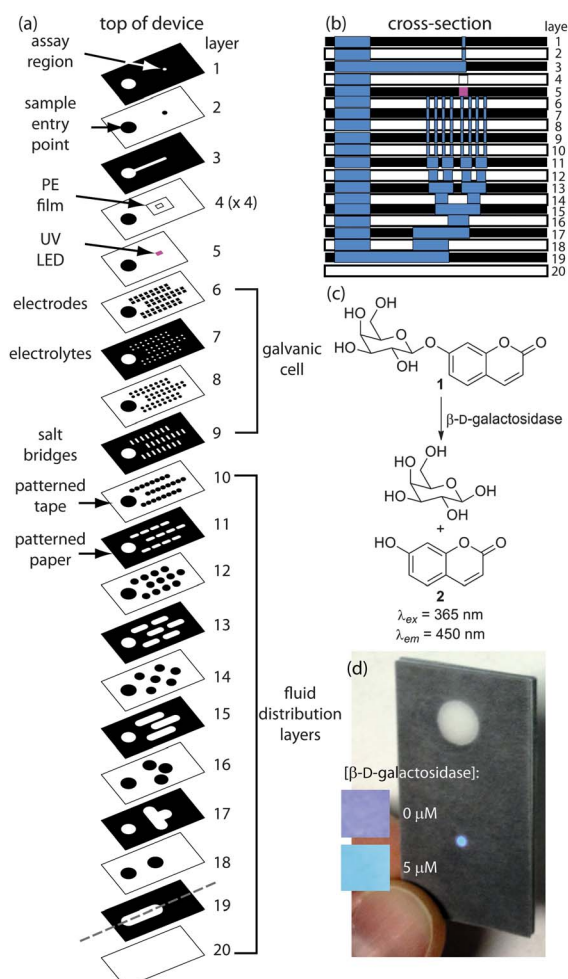


**Fig. 2** A fluorescent assay on a paper-based microfluidic device for detecting  $\beta$ -D-galactosidase. (a) Expanded view of the device. The device contains an inlet for a sample, and a readout region that emits 450-nm light if the analyte is in the sample. The fluidic battery powers an integrated surface-mount UV LED that illuminates the assay region. (b) Cross-section of the device in (a) showing the distribution of sample (blue) within one section of the device. The location of the cross-section is depicted in layer 19 in (a). (c) Reagent **1** is pre-deposited into the assay region prior to assembling the device. Reagent **1** selectively reacts with  $\beta$ -D-galactosidase through an activity-based detection event that releases 7-hydroxycoumarin (**2**). Reagent **1** is not fluorescent, whereas **2** is highly fluorescent. (d) “Colorimetric” output provided by the on-chip fluorescence assay as a function of the concentration of  $\beta$ -D-galactosidase in the sample. The assay time was 19 min for both the 0 and 5  $\mu\text{M}$   $\beta$ -D-galactosidase samples (see the inset images). The 5- $\mu\text{M}$  inset is an expanded view of the larger photograph. The volume of sample added to the device was 350  $\mu\text{L}$ .

(including the fluorescent dye 7-hydroxycoumarin (**2**)) when **1** reacts with  $\beta$ -D-galactosidase, which is a general marker for fecal contamination in water.<sup>8</sup> Compound **1** was pre-deposited onto the assay region in layer 1 prior to assembling the device.

In 100  $\mu$ M phosphate-buffered water (pH 7.2) (100 mM buffer) containing 0.16% DMSO, 7-hydroxycoumarin has a maximum excitation wavelength of 365 nm and emits at 450 nm, making it suitable to pair with the UV LED ( $\lambda_{\text{em}} = 375 \pm 5$  nm). This assay provides a bright blue signal that can be imaged using a camera-equipped cellular phone. The UV LED is arranged such that the UV light is projected up through a 50- $\mu$ m thick, 4 mm  $\times$  5 mm rectangular sheet of polyethylene (PE) (which is included to protect the UV LED from moisture) and two layers of 180- $\mu$ m thick Whatman Chromatography paper No. 1 before the light reaches and passes through the detection zone in layer 1 (which is made of 180- $\mu$ m thick Whatman Chromatography paper No. 1) (Fig. 2a). Layer 4 in Fig. 2a is repeated four times, and contains a 2.5 mm  $\times$  3.5 mm hole in the tape, which provides a protective compartment that surrounds the surface-mount LED that is affixed to layer 5 using copper tape.

The UV LED in Fig. 2a emits a consistent intensity of light when  $\geq 3.12$  V and  $\geq 105$   $\mu$ A are generated in the fluidic battery (Fig. S9). This level of voltage and current is reached within 17 min of adding a sample to the device, and is maintained for 21 min (see the bracket in Fig. S9), which provides, in total, a 38 min window for the assay reagents (*i.e.*, reagent **1**, Fig. 2c) to generate a detectable level of 7-hydroxycoumarin in the assay region.

Fig. 2d provides a proof-of-concept demonstration that the device shown in Fig. 2a is capable of detecting  $\beta$ -D-galactosidase in a sample of water. To ensure an appropriate pH value for the on-chip assay, we pre-deposited 0.2  $\mu$ L of 100 mM sodium phosphate buffer solution (pH 7.2) into the 1.2-mm diameter hydrophilic piece of paper located in layer 1. This wet region of layer 1 was dried prior to assembling the device. As the sample wicks to the assay region, it redissolves the buffer salts to create a pH 7.2 solution to account for samples of water that vary in pH and to normalize the rate of the enzymatic assay. Exposure of individual devices at 21 °C to water containing two different quantities of  $\beta$ -D-galactosidase yielded strikingly different fluorescent responses when viewed 19 min after adding the sample to the device, as depicted in Fig. 2d. Because three layers of paper were placed over the UV LED in the device, the visible purple light emitted by the LED is diminished in intensity, but a faint hue of purple remains, as shown in the inset of Fig. 2d for 0  $\mu$ M  $\beta$ -D-galactosidase. The presence of 5  $\mu$ M  $\beta$ -D-galactosidase, however, provides a vivid blue color in the assay region, as depicted in both the large photograph and the inset.

## Conclusions

We believe that several features of the fluidic batteries make them particularly well-suited for diagnostics in resource-limited settings: (i) the batteries generate power directly in line with assays; (ii) they “turn on” upon addition of a sample to the device; (iii) the number of galvanic cells that make up the battery can be increased or decreased easily; and (iv) the configuration of the galvanic cells relative to one

another is easily altered. The latter two features control the current and voltage of the fluidic battery, and can be reconfigured to optimize a device so that the minimum quantity of metal electrodes and electrolytes are used for a particular assay. In theory, such capabilities should now make it possible to disconnect paper microfluidic devices from externally-powered readers, even when running complex assays. In their current form, the fluidic batteries require from 8  $\mu$ L to 350  $\mu$ L of sample depending on the configuration of the channels in the devices, the assay that is run, and the power needed from the battery. Optimized designs should easily shrink these volume requirements further. The initial development of paper microfluidics was motivated by the need for low-cost and easy to use diagnostic platforms that do not require external equipment (*e.g.*, pumps);<sup>2</sup> we believe that these fluidic batteries complement this philosophy and will enable the rapid advancement of paper microfluidics, particularly as more sophisticated (and often more useful) assays are integrated into the paper microfluidic platform.

## Acknowledgements

This work was supported in part by the Bill and Melinda Gates Foundation as a subcontract from Harvard University (Subcontract No. 01270716-00), 3M, Mr. Louis Martarano, and The Pennsylvania State University. We thank Dr Landy K. Blasdel for assistance in preparing the manuscript.

## Notes and references

- 1 P. P. Yager, T. Edwards, E. Fu, K. Helton, K. Nelson, M. R. Tam and B. H. Weigl, *Nature*, 2006, **442**, 412; M. Urdea, L. A. Penny, S. S. Olmsted, M. Y. Giovanni, P. Kaspar, A. Shepherd, P. Wilson, C. A. Dahl, S. Buchsbaum, G. Moeller and D. C. Hay Burgess, *Nature*, 2006, **S1**, 73.
- 2 A. W. Martinez, S. T. Phillips, G. M. Whitesides and E. Carrilho, *Anal. Chem.*, 2010, **82**, 3; H. Liu and R. M. Crooks, *J. Am. Chem. Soc.*, 2011, **133**, 17564; Z. Nie, C. A. Nijhuis, J. Gong, X. Chen, A. Kumachev, A. W. Martinez, M. Narovlyansky and G. M. Whitesides, *Lab Chip*, 2010, **10**, 477; S. N. Tan, L. Ge and W. Wang, *Anal. Chem.*, 2010, **82**, 8844; M. M. Ali, S. D. Aguirre, Y. Xu, C. D. M. Filipe, R. Pelton and Y. Li, *Chem. Commun.*, 2009, 6640; W. Dungchai, O. Chailapakul and C. S. Henry, *Anal. Chem.*, 2009, **81**, 5821; J. L. Delaney, C. F. Hogan, J. Tian and W. Shen, *Anal. Chem.*, 2011, **83**, 1300.
- 3 R. W. Peeling, K. K. Holmes, D. Mabey and A. Ronald, *Sex. Transm. Infect.*, 2006, **82**, v1.
- 4 For leading general references on batteries in paper see: K. B. Lee, *J. Micromech. Microeng.*, 2005, **15**, S210; K. B. Lee, *J. Micromech. Microeng.*, 2006, **16**, 2312; L. Nyholm, G. Nyström, A. Mihranyan and M. Strømme, *Adv. Mater.*, 2011, **23**, 3751.
- 5 Five weeks was the maximum length of time that we tested the devices.
- 6 On a per cell basis, the cost of materials is approximately \$0.00000009 for  $\text{AlCl}_3$ , \$0.0002 for  $\text{AgNO}_3$ , \$0.0009 for aluminum metal, \$0.015 for silver metal, and \$0.000002 for  $\text{NaNO}_3$ . The estimated cost of materials for a single cell fluidic battery is \$0.017, while the four cell designs shown in Figs. 1c and 1d cost approximately \$0.066 each. Future designs using less expensive metals will reduce these values further.
- 7 Other configurations of the cells are possible, but these examples clearly demonstrate the broad range of  $I_{\text{sc}}$  and  $V_{\text{oc}}$  values that are possible with this type of fluidic battery.
- 8 I. Tryland and L. Fiksdal, *Appl. Environ. Microbiol.*, 1998, **64**, 1018.